

# Circulating sphingolipid biomarkers in models of type 1 diabetes

Todd E. Fox,<sup>\*,†</sup> Maria C. Bewley,<sup>§</sup> Kellee A. Unrath,<sup>\*</sup> Michelle M. Pedersen,<sup>\*</sup> Robert E. Anderson,<sup>\*\*</sup> Dae Young Jung,<sup>†</sup> Leonard S. Jefferson,<sup>†</sup> Jason K. Kim,<sup>†</sup> Sarah K. Bronson,<sup>†</sup> John M. Flanagan,<sup>§</sup> and Mark Kester<sup>1,\*</sup>

Departments of Pharmacology,<sup>\*</sup> Cellular & Molecular Physiology,<sup>†</sup> and Biochemistry and Molecular Biology,<sup>§</sup> Penn State College of Medicine, Milton S. Hershey Medical Center, Hershey, PA; and Dean A. McGee Eye Institute and Department of Ophthalmology,<sup>\*\*</sup> University of Oklahoma Health Sciences Center, Oklahoma City, OK

**Abstract** Alterations in lipid metabolism may contribute to diabetic complications. Sphingolipids are essential components of cell membranes and have essential roles in homeostasis and in the initiation and progression of disease. However, the role of sphingolipids in type 1 diabetes remains largely unexplored. Therefore, we sought to quantify sphingolipid metabolites by LC-MS/MS from two animal models of type 1 diabetes (streptozotocin-induced diabetic rats and Ins2<sup>Akita</sup> diabetic mice) to identify putative therapeutic targets and biomarkers. The results reveal that sphingosine-1-phosphate (So1P) is elevated in both diabetic models in comparison to respective control animals. In addition, diabetic animals demonstrated reductions in plasma levels of omega-9 24:1 (nervonic acid)-containing ceramide, sphingomyelin, and cerebroside. Reduction of 24:1-esterified sphingolipids was also observed in liver and heart. Nutritional stress via a high-fat diet also reduced 24:1 content in the plasma and liver of mice, exacerbating the decrease in some cases where diabetes was also present. Subcutaneous insulin corrected both circulating So1P and 24:1 levels in the murine diabetic model. Thus, changes in circulating sphingolipids, as evidenced by an increase in bioactive So1P and a reduction in cardio- and neuro-protective omega-9 esterified sphingolipids, may serve as biomarkers for type 1 diabetes and represent novel therapeutic targets.—Fox, T. E., M. C. Bewley, K. A. Unrath, M. M. Pedersen, R. E. Anderson, D. Y. Jung, L. S. Jefferson, J. K. Kim, S. K. Bronson, J. M. Flanagan, and M. Kester. **Circulating sphingolipid biomarkers in models of type 1 diabetes.** *J. Lipid Res.* 2011. 52: 509–517.

**Supplementary key words** nervonic acid • sphingosine-1-phosphate • ceramide • sphingomyelin • cerebroside • lipidomics

Diabetes is a debilitating chronic disease that has no cure and can only be managed by pharmaceutical and/or nutritional interventions. Worldwide, the incidence of diabetes and diabetic complications is dramatically increasing, possibly due to a worldwide obesity epidemic. It is argued that although targeting obesity will radically decrease the incidence and complications of type 2 diabetes, no such general nutritional solution exists for patients with type 1 diabetes. Yet patients with type 1 diabetes who adhere to the American Diabetes Association diet guidelines and/or exhibit a low body mass index demonstrate significant reductions in complications. Despite the knowledge that altered lipid metabolism is a cardinal feature of both type 1 and 2 diabetes, the actual lipid species that contribute to complications such as diabetic nephropathy, retinopathy, neuropathy, and cardiovascular disease have not been comprehensively studied in type 1 models and may offer a targeted nutritional approach for these patients.

Although sphingolipids comprise only a fraction of total lipids, a body of evidence has now identified dysfunctional sphingolipid metabolism and generation of specific sphingolipid metabolites as contributors to diabetic complications (1). Most of the evidence pointing to a role of sphingolipids in diabetes has utilized models of type 2 diabetes. Treatment of Zucker fa/fa rats and diet-induced obese mice with the de novo sphingolipid inhibitor, myriocin, improved glucose tolerance and insulin sensitivity (2). Similarly, treatment strategies that inhibit glucosylceramide synthase have proven effective in diabetic animal

Research was supported by the Pennsylvania (PA) Department of Health using Tobacco Settlement Funds as well as a Juvenile Diabetes Research Foundation postdoctoral fellowship (to T.E.F.). In addition, research was supported by National Eye Institute NEI EY018336 and American Diabetes Association Research Award (to M.K.) and 7-07-RA-80 (to J.K.K.). Core Facility services and instruments (ABI 4000 QTrap) used in this project were funded, in part, under a grant with the Pennsylvania Department of Health using Tobacco Settlement Funds. The Department specifically disclaims responsibility for any analyses, interpretations, or conclusions.

Manuscript received 16 August 2010 and in revised form 9 November 2010.

Published, JLR Papers in Press, November 10, 2010

DOI 10.1194/jlr.M010595

Abbreviations: Sa, sphinganine, Sa1P, sphinganine-1-phosphate; So, sphingosine; So1P, sphingosine-1-phosphate; STZ, streptozotocin.

<sup>1</sup>To whom correspondence should be addressed.

e-mail: mkester@psu.edu

models. Treatment of obese (*ob/ob*) mice with the selective glucosylceramide synthase inhibitor, *N*-(5-Adamantane-1-yl-methoxy-pentyl)-deoxynojirimycin, lowered blood glucose levels, improved oral glucose tolerance, reduced hemoglobin A1c, and improved insulin sensitivity in muscle and liver (3). Similar beneficial metabolic effects were observed in high-fat-fed mice and Zucker rats (3). Diminished blood glucose, improved glucose tolerance, and reduced A1c levels were also observed with a structurally distinct glucosylceramide synthase inhibitor, Genz-123346, in Zucker diabetic fatty rats and diet-induced obese mice. This inhibitor also limited the loss of pancreatic  $\beta$ -cell function, suggesting that sphingolipid metabolism might be affected in type 1 diabetes (4). Although these studies have demonstrated therapeutic efficacy in modulating sphingolipid metabolism, the actual diabetes-induced changes in sphingolipids remain poorly characterized.

Herein, we analyzed the circulating sphingolipids in two distinct models of type 1 diabetes, the streptozotocin (STZ)-induced diabetic rat and the *Ins2<sup>AKita</sup>* diabetic mouse. We also determined the sphingolipid profile of *Ins2<sup>AKita</sup>* mice in the presence or absence of nutritional “stress” (high-fat diet) and the effects of subcutaneous-implanted delivery of insulin to correct dysfunctional sphingolipid metabolism in the murine model.

## MATERIALS AND METHODS

### Materials

All lipid standards were obtained from Avanti Polar Lipids (Alabaster, AL). All solvents were HPLC grade or higher and obtained from Thermo Fisher Scientific (Waltham, MA) or Honeywell Burdick and Jackson (Morristown, NJ).

### Animals

Male *Ins2<sup>AKita</sup>* mice and wild-type littermates (C57BL/6J background) were housed under controlled temperature and a 12 h light/dark cycle with free access to food (Teklad 2019) and water (5). The Akita allele is a spontaneous, dominantly inherited mutation in one of the two mouse insulin genes. The *Ins2<sup>AKita</sup>* mutation arose on the C57BL/6 background and upon transfer to The Jackson Laboratory (JAX) was bred to C57BL/6J. We imported the line from JAX and have continuously maintained the line by breeding to C57BL/6J stock. *Ins2<sup>AKita/+</sup>* male mice are bred to *Ins2<sup>+/+</sup>* female stock mice to generate the experimental male littermates, *Ins2<sup>AKita/+</sup>* (*Ins2<sup>AKita</sup>*) and *Ins2<sup>+/+</sup>* (wild-type). All mice were housed under controlled temperature and a 12 h light/dark cycle with free access to food (Teklad 2019) and water. *Ins2<sup>AKita</sup>* mice demonstrate increased food intake, increased energy expenditure (despite being less active), and a significant reduction in respiratory exchange ratio (5). For some studies (see Table 1 for details), animals at about 12 weeks of age (~8 weeks hyperglycemia), were switched to a high-fat diet (Teklad 93075) for 6 weeks. Whole body fat and lean mass were noninvasively measured in awake *Ins2<sup>AKita</sup>* and wild-type mice at 14 weeks of age using <sup>1</sup>H-MRS (Echo Medical Systems, Houston, TX). Some *Ins2<sup>AKita</sup>* diabetic mice received continuous insulin treatment via subcutaneous implant of LinBit pellets (LinShin, Canada, Inc.) 6 weeks prior to harvest following the manufacturer’s instructions (3–4 pellets/animal determined by animal weight). Blood glucose concentrations and percent glycosylated hemoglo-

bin were measured from drops of blood acquired by nicking the tail using a Lifescan glucose meter and Siemens DCA Analyzer, respectively. Cartridges for the quantitative measurement of hemoglobin A1c are based on specific monoclonal antibody agglutination.

Male Sprague-Dawley rats (Charles River Laboratories, Wilmington, MA) were fasted overnight and given a single intraperitoneal injection of STZ (65 mg/kg; Sigma-Aldrich, St. Louis, MO) freshly dissolved in 10 mmol/l sodium citrate buffer (pH 4.5) (6). Diabetes was confirmed 6 days later by blood glucose > 250 mg/dl (Lifescan, Milpitas, CA). Age-matched control and diabetic rats were monitored regularly by weight and blood glucose tests. Rats were group-housed in solid plastic-bottom cages with bedding as well as ad libitum food (Teklad Global 18% protein rodent diet) and water under a normal 12 h light/dark schedule.

Animals were maintained by the Juvenile Diabetes Research Foundation Animal Core Facility at Pennsylvania State University in accordance with the institutional animal care and use committee guidelines. The average weight and blood glucose level of each animal was recorded on the day they were euthanized and are indicated in Table 1. All procedures were approved by the Pennsylvania State University Institutional Animal Care and Use Committee.

### Sphingolipid analyses

Sphingolipids were analyzed by LC/ESI-MS/MS based on the method described by Merrill et al. (7) with some modifications (8). These modifications ensure that the samples are properly neutralized to prevent breakdown of sphingomyelin and lysosphingomyelin into other lipids if dried under alkaline conditions (8). Lipids from heparinized plasma (25  $\mu$ l), liver (500  $\mu$ g protein), and heart (500  $\mu$ g protein) were extracted and separated on an Agilent 1100 HPLC system. Mobile phases were as described (7), but with 0.2% formic acid on a Luna C8 (3  $\mu$ ) 2mm ID  $\times$  5cm column maintained at 60°C for separation of the

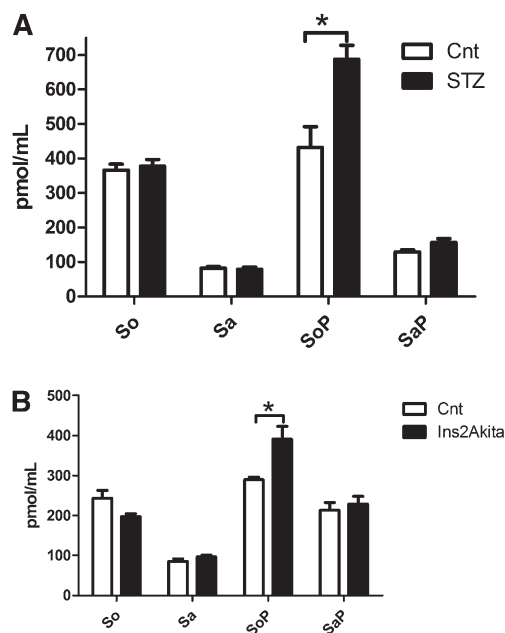


**Fig. 1.** So1P is increased in the diabetic plasma. Sphingolipid long-chain bases were measured by LC-MS/MS from (A) 4 week STZ-induced diabetic rats and age-matched controls and (B) 14-week old *Ins2<sup>AKita</sup>* mice and nondiabetic sibling controls (shown as pmol/ml). n values are provided in Table 1. \**P* < 0.01.

sphingoid bases and 1-phosphates. The eluate was analyzed with an inline ABI 4000 Q Trap (Applied Biosystems, Foster City, CA) mass spectrometer equipped with a turbo ion spray source. The peak areas for the different sphingolipid subspecies were compared with that of the internal standards. All data reported are based on monoisotopic mass and are represented as pmol/ml for plasma and pmol/mg protein for heart and liver tissue.

### Fatty acid derivatization and gas-liquid chromatography

Total lipids were extracted for fatty acid analysis from plasma as described previously (9). Total lipid extracts were then converted to methyl esters by addition of 2% H<sub>2</sub>SO<sub>4</sub> in methanol and heated at 100°C for 65 min. A mixture of pentadecanoic acid (15:0), heptadecanoic acid (17:0), and heneicosanoic acid (21:0) were added as internal standards. Tubes were cooled on ice and fatty acid methyl esters were extracted three times with hexane, dried under N<sub>2</sub>, and dissolved in nonane. The fatty acid compositions were determined by injecting 3 μL of each sample at 250°C

with the split ratio set to 20:1 using a DB-225 capillary column (30 m × 0.53 mm inner diameter; J and W Scientific, Folsom, CA) in a gas-liquid chromatograph (model 6890N; Agilent Technologies, Wilmington, DE) and an autosampler (model 7683; Agilent Technologies). The column temperature was programmed to hold at 160°C for 1 min, then increased to 220°C at 1°C/min, and held at 220°C for 10 min. Helium carrier gas flowed at 4.2 ml/min. The hydrogen flame ionization detector temperature was set to 270°C. The chromatographic peaks were integrated and processed on computer (ChemStation software; Agilent Technologies). Fatty acid methyl esters were identified by comparing their relative retention times with authentic standards, then their relative mol percentages were calculated.

### Statistical methods

Statistical analyses (*t*-tests) were performed using GraphPad Prism 4.0 software, with statistical significance considered if *P* < 0.05.

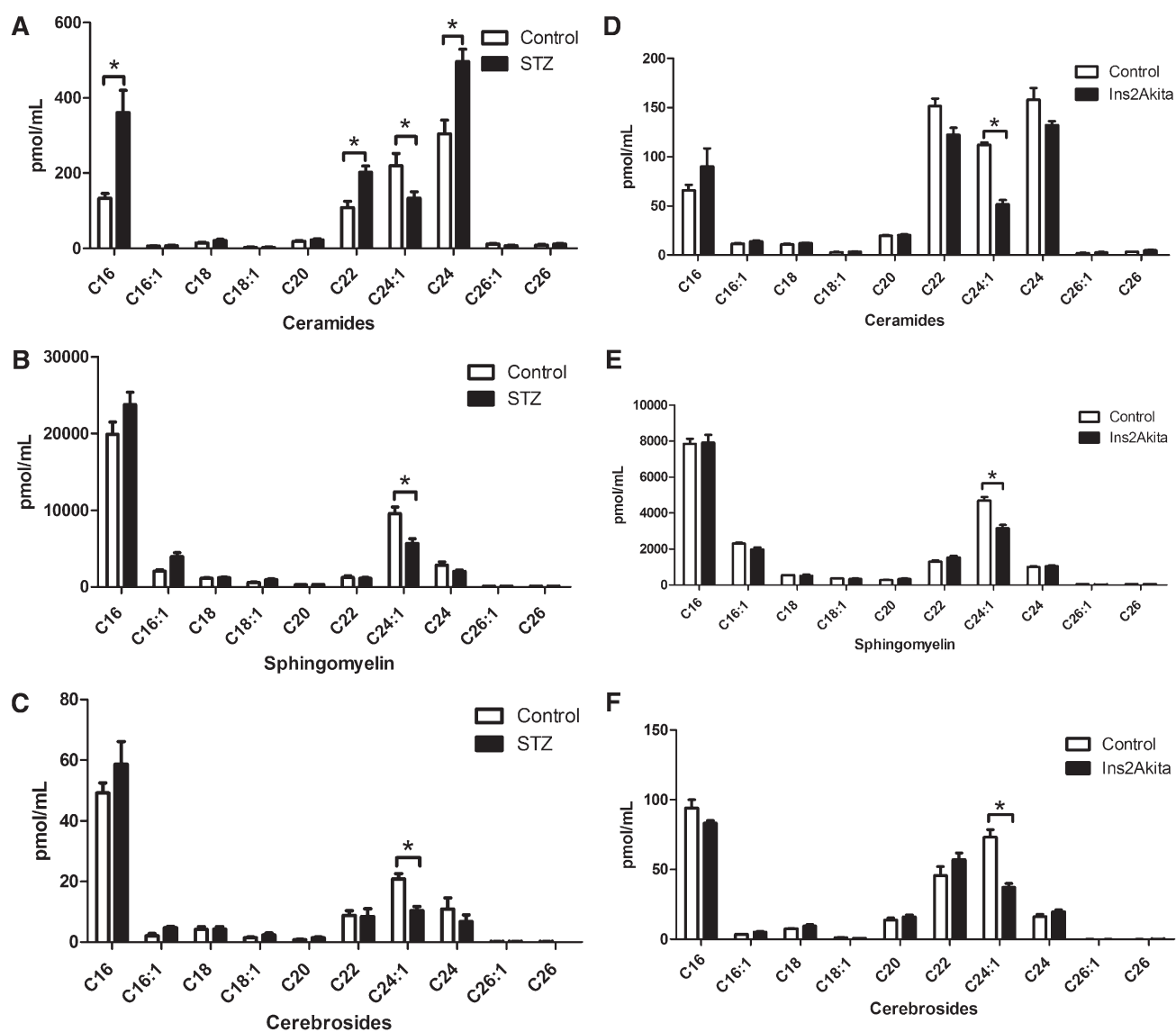


**Fig. 2.** Fatty-acid esterified sphingolipids are altered in the plasma from diabetic models. The ceramide, sphingomyelin, and cerebroside classes of sphingolipids were measured by LC-MS/MS from 4-week STZ-induced diabetic rats (A, ceramides; B, sphingomyelin; C, cerebrosides) and age-matched controls as well as 14-week-old Ins2<sup>Akita</sup> mice and nondiabetic sibling controls (D, ceramides; E, sphingomyelin; F, cerebrosides). Values are shown as pmol/ml; *n* values are provided in Table 1. \**P* < 0.01.

## RESULTS

### Plasma sphingolipid profiling of the *Ins2<sup>Akita</sup>* diabetic mouse and STZ-induced diabetic rat reveals altered sphingolipid metabolites

Due to the rising importance of sphingolipids as contributors to the pathogenesis of various disease processes (10), we sought to obtain a better understanding of diabetes-induced changes of sphingolipids in models of type 1 diabetes. We initially assessed the sphingolipid profile from lipids extracted from the plasma of the STZ-diabetic rat, a drug-induced diabetic model, and the *Ins2<sup>Akita</sup>* mouse, a genetic model of diabetes. *Ins2<sup>Akita</sup>* mice contain a dominant mutation in the insulin 2 gene, which causes a conformational change that induces the unfolded protein response. This, in turn, results in pancreatic  $\beta$ -cell death and subsequent spontaneous induction of diabetes within 4 weeks of birth (11). Utilizing LC-MS/MS, we quantified the long-chain bases: sphingosine-1-phosphate (So1P), sphinganine-1-phosphate (Sa1P), sphingosine (So), and sphinganine (Sa). Elevated levels of So1P were observed in both STZ-treated rats (**Fig. 1A**) (34.7%) and *Ins2<sup>Akita</sup>* mice (**Fig. 1B**) (29.8%), relative to their controls. Interestingly, the dihydro form, Sa1P, was unaltered as were the metabolic precursors, So and Sa.

The fatty acid-esterified sphingolipid molecular species of ceramides, cerebroside, and sphingomyelin were also quantified in the plasma. Specifically, we observed that the C16:0, C22:0, and C24:0 fatty acid-esterified ceramides were elevated in the STZ-induced diabetic rat (**Fig. 2A**), but not in the *Ins2<sup>Akita</sup>* mouse (**Fig. 2D**). It is unclear if this difference is due to a secondary toxic effect of the STZ or due to differences in the models. For example, STZ-diabetic rats are typically hyperlipidemic and *Ins2<sup>Akita</sup>* have higher basal insulin levels. Further examination of the fatty acid profiles of both models revealed a significant decrease in the omega-9, 24:1 fatty acid (nervonic acid). Nervonyl-containing ceramides decreased 60.6% in the STZ-induced diabetic rat model and 53.4% in the *Ins2<sup>Akita</sup>* model. This decrease was also observed in the sphingomyelin [STZ

(**Fig. 2B**) and *Ins2<sup>Akita</sup>* (**Fig. 2E**)] and cerebroside [STZ (**Fig. 2C**) and *Ins2<sup>Akita</sup>* (**Fig. 2F**)] classes of sphingolipids. Besides the decreased 24:1 molecular species, there were no other fatty acyl changes in the sphingomyelin or cerebroside classes of sphingolipids. It should be noted that the levels of cerebroside in the plasma are appreciably lower relative to other lipids.

### High-fat feeding decreases 24:1-containing sphingolipids

To examine the effects of nutritional stress, wild-type and *Ins2<sup>Akita</sup>* mice were fed a high-fat diet for 10 weeks. This high-fat diet has been utilized frequently in the literature as a model for diet-induced obesity in C57BL/6J mice (12–15). After this time, *Ins2<sup>Akita</sup>* mice gained, on average, 1.3 g of fat compared with wild-type mice, which gained on average 6.3 g (**Table 1**). Likewise, *Ins2<sup>Akita</sup>* mice were resistant to a high-fat diet-induced increase in body weight, consistent with type 1 diabetes. On the high-fat diet, *Ins2<sup>Akita</sup>* diabetic as well as wild-type mice showed significant decreases in nervonic acid for ceramide (**Fig. 3A**), sphingomyelin (**Fig. 3B**), and cerebroside (**Fig. 3C**). In diabetics, the decrease in 24:1 containing sphingomyelin and cerebroside classes was exacerbated with the high-fat diet. These data demonstrate that both a high-fat diet and diabetes result in significant decreases of nervonic acid-containing sphingolipids.

### Insulin treatment corrects altered So1P and C24:1 content in plasma sphingolipids

We next determined whether insulin therapy could restore these selective alterations in So1P and C24:1 induced by diabetes. *Ins2<sup>Akita</sup>* mice were given subcutaneous insulin implants for 6 weeks. This insulin treatment decreased blood glucose levels and hemoglobin A1c levels in *Ins2<sup>Akita</sup>* mice (**Table 1**). We again analyzed the sphingolipid content from the plasma of these animals. As previously seen, the diabetic animals showed a significant increase in So1P levels (**Fig. 4A**), and those treated with insulin showed a return of So1P to basal levels. We also report that insulin treatment in

TABLE 1. Animal information

Study	Group	n	Weight (g)	Blood Glucose (mg/dl)	HbA1C (%)	Body Fat (g)
Figs. 1A, 2A–C	Control (4wk)	8	422.8 ± 8.4	98.8 ± 3.6		
	Diabetic (STZ - 4wk)	7	277.8 ± 16.2	420.9 ± 19.9		
Figs. 1B, 2D–F, 3	Wild-type (14wk)	10	28.5 ± 0.5	194 ± 6.9		3.9 ± 0.2
	<i>Ins2<sup>Akita</sup></i> (14wk)	7	25.1 ± 0.6	Above limit		3.2 ± 0.1
	Wild-type + High Fat	11	33 ± 1.1	212 ± 15.3		10.2 ± 1.0
	<i>Ins2<sup>Akita</sup></i> + High Fat	10	25.6 ± 0.4	512 ± 23.2		4.5 ± 0.1
Figs. 4, 6	Wild-type (16 wk)	7	28.4 ± 1.5	223 ± 16.9	4.4 ± 0.09	
	<i>Ins2<sup>Akita</sup></i> (16 wk)	7	22.3 ± 0.6	382 ± 50.6	13.3 ± 0.26	
	<i>Ins2<sup>Akita</sup></i> + insulin (16wk)	7	25.2 ± 0.5	Above limit	6.7 ± 0.31	
Fig. 5	Control (4wk)	7	391.1 ± 14.7	108.6 ± 4.3		
	Diabetic (STZ-4wk)	7	303.6 ± 9.6	409.3 ± 17.6		
Fig. 7	Wild-type (14wk)	10	27.1 ± 0.4	168 ± 6.2		4.0 ± 0.2
	<i>Ins2<sup>Akita</sup></i> (14wk)	9	24.9 ± 0.7	533 ± 23.2		3.0 ± 0.1
	Wild-type + High Fat	10	35.4 ± 1.35	161 ± 4.1		11.8 ± 0.9
	<i>Ins2<sup>Akita</sup></i> + High Fat	10	25.7 ± 0.2	452 ± 22.0		4.4 ± 0.2

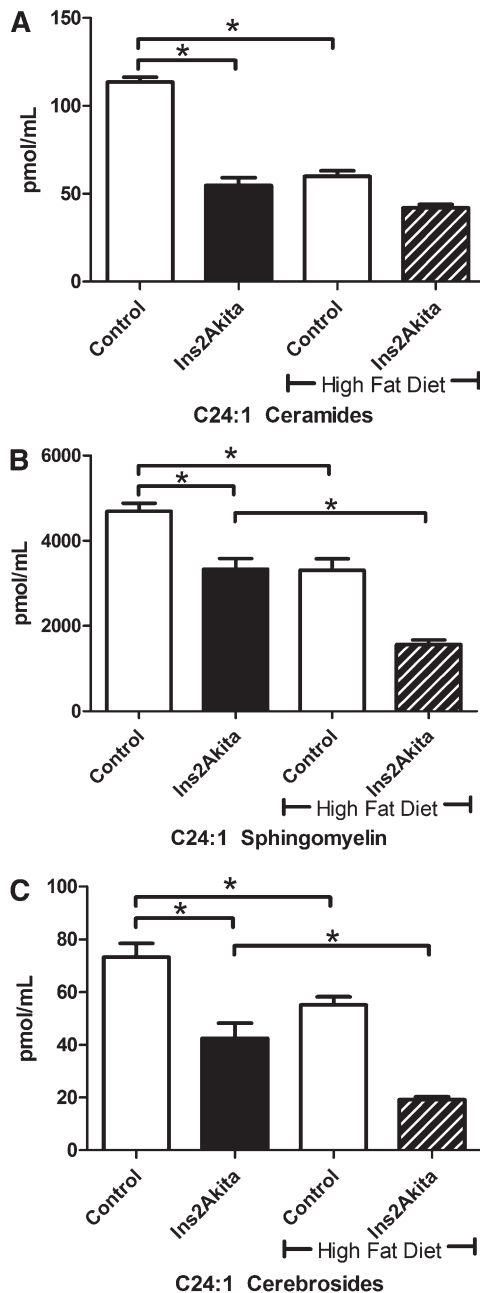


**Fig. 3.** A high-fat diet reduces 24:1 containing sphingolipids in the plasma. Ten-week-old  $Ins2^{Akita}$  diabetic mice and nondiabetic mice were fed a high-fat diet for 6 weeks. Plasma was collected and analyzed by mass spectrometry for 24:1-esterified (A) ceramides, (B) sphingomyelin, and (C) cerebrosides (data shown as pmol/ml); n values are provided in Table 1. \* $P < 0.05$ .

diabetic animals restores 24:1 levels to that of controls for ceramide (Fig. 4B) and sphingomyelin (data not shown).

#### Plasma fatty acid analysis

To further confirm this diminished 24:1 fatty acid content of esterified sphingolipids from the plasma, we analyzed the fatty acid profile of the total lipids present in the plasma of the STZ-induced diabetic rat. By gas chromatography-flame ionization detector (GC-FID) analysis of total fatty acids, we observed diminished 24:1 nervonic acid (Fig. 5 inset). Interestingly, whereas the percentage of 24:1 in

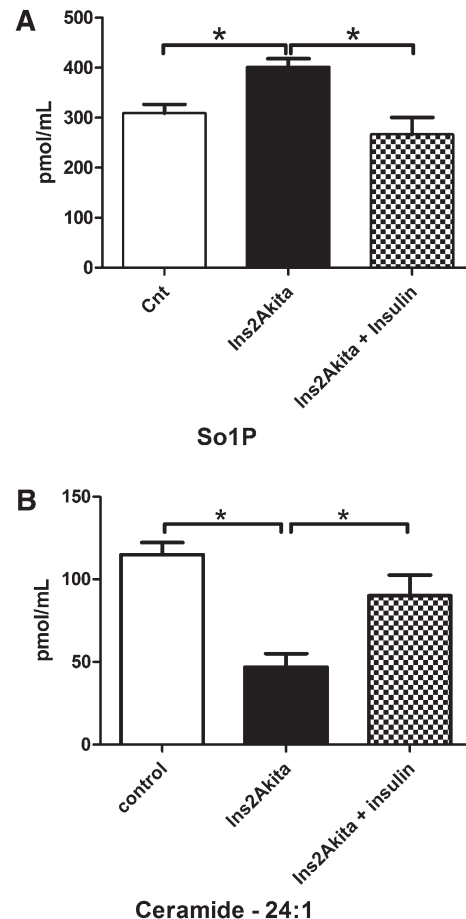


**Fig. 4.** Insulin treatment restores diabetes induced sphingolipid changes in the plasma. Ten-week-old  $Ins2^{Akita}$  diabetic mice were administered insulin via subcutaneous insulin pellets for an additional 6 weeks. A: So1P content was measured from the plasma from control,  $Ins2^{Akita}$ , and insulin-treated  $Ins2^{Akita}$ . B: Similarly, 24:1-containing ceramides were also assessed (data shown as pmol/ml); n values are provided in Table 1. \* $P < 0.05$ .

free or esterified form is relatively low compared with other fatty acids in the total lipid pool, the percentage of 24:1 present on sphingolipid classes is considerably higher (Fig. 2). This suggests that nervonic acid is selectively esterified to sphingolipids rather than glycerol-containing lipids. We also observe that metabolic precursors to omega-9 24:1, specifically 16:1 and 18:1, are significantly decreased in diabetics, in contrast to increases in 18:0 and 18:2 omega-6 fatty acyl precursors (Fig. 5). Also of interest, this elevation of 18:2 does not get further metabolized to 20:4n6 (arachidonic acid). Overall, these data demonstrate that diabetes results in the selective decrease in omega-9 fatty acids.

#### Sphingolipids in the heart

Because both elevated So1P levels and diminished nervonic acid have been correlated with cardiovascular complications (16, 17), sphingolipid molecular species were also assessed from heart tissue of wild-type and  $Ins2^{Akita}$  diabetic mice. Clinical data have shown that circulating So1P is predictive of obstructive coronary artery disease (16). In addition, it has been reported that nervonic acid exerts a negative correlation on coronary risk factors and consequently, may

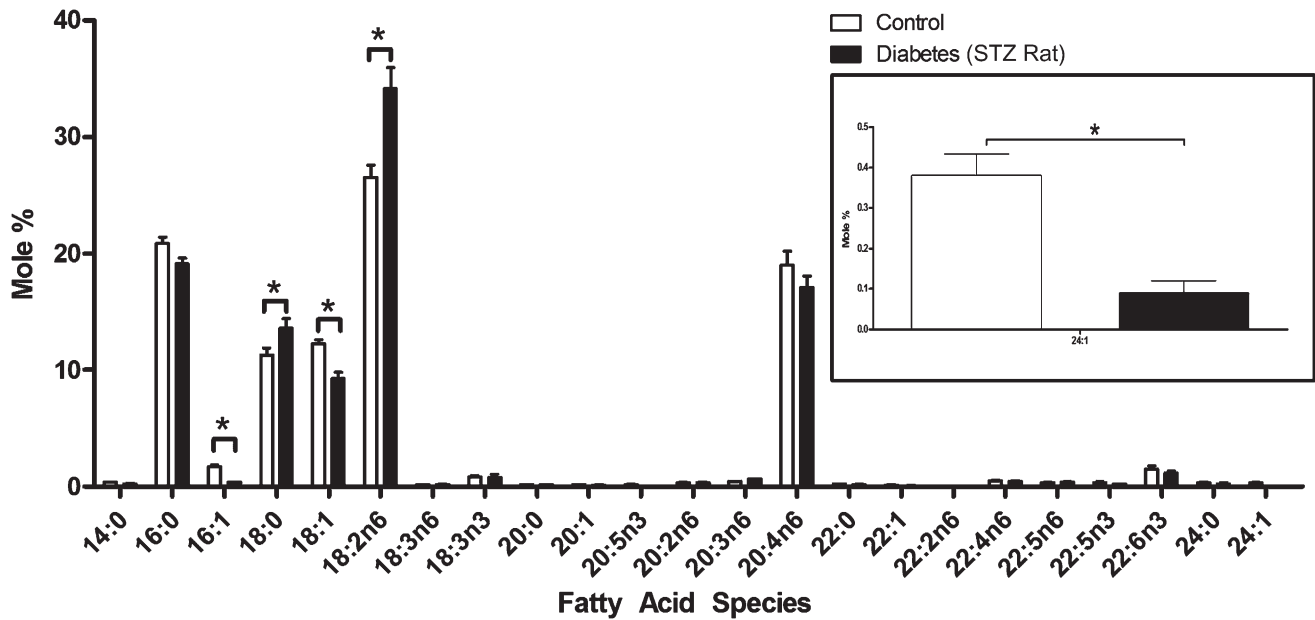


**Fig. 5.** Plasma fatty acid content is altered with diabetes. Total lipids from the plasma of control and diabetic animals were derivatized to methyl esters and analyzed by GC-FID. The mol% of each fatty acid is shown. The 24:1 values are shown in the inset. Significance is indicated by a \* ( $P < 0.05$ ) and n values are provided in Table 1.

have a preventative effect on cardiovascular disorders (17). Nervonic acid constitutes a much smaller proportion of the fatty-esterified sphingolipids in the heart as compared with the plasma. However, we again observed a significant reduction in nervonic acid-containing ceramides (Fig. 6A) and sphingomyelin (data not shown) without alterations in other fatty acids. In these animals, we also assessed the ability of insulin therapy, by means of a subcutaneous implant, to alter nervonic acid-containing sphingolipids. As we have observed in the plasma, insulin was again able to rescue this decrease in nervonic acid-containing sphingolipids.

We also assessed SoIP levels in the wild-type and diabetic  $Ins2^{Akit1}$  heart tissue (Fig. 6B). As in the plasma, a significant increase in SoIP levels was observed in diabetic heart tissue. Insulin treatment, although not significantly different, reduced SoIP levels in five out of seven animals. Other sphingolipids, So and Sa, were not altered by diabetes (data not shown). These data demonstrate that the heart has a similar response to diabetes as the plasma.

### Sphingolipid profile of the diabetic liver

Because sphingolipids can be packaged onto lipoprotein complexes in the plasma, this potentially implicates the liver as a contributory factor in altered sphingolipids in circulation. We observed several diabetes-induced changes in the liver tissue of the  $Ins2^{Akit1}$  diabetics. Increases in the saturated 16:0 and 18:0 ceramides were observed (Fig. 7A). Also, a decrease in 24:1 containing ceramides was observed, as previously seen in the plasma. This reduction in nervonic acid again reveals it is not specific to ceramides. Both diabetes and a high-fat diet reduced the nervonic acid content of the sphingomyelin (Fig. 7B) and cerebroside (Fig. 7C) classes of sphingolipids. We again observe a cooperative effect of a high-fat diet on reducing 24:1 in diabetic animals. It

should be noted again that cerebroside content is considerably less than other esterified sphingolipids. Taken together, this data suggests that reduced 24:1 containing sphingolipids in circulation may be a consequence of altered liver sphingolipid metabolism.

We also evaluated SoIP levels in the liver tissue of the  $Ins2^{Akit1}$  diabetic model. Here, we did not observe changes in liver SoIP in diabetic animals (Fig. 7D). The lack of diabetes-induced SoIP changes suggests a different source of elevated SoIP.

## DISCUSSION

Although defective insulin signaling and hyperglycemia are the major underlying factors for diabetes and its complications, alterations to the metabolites that contribute to a homeostatic environment are still poorly defined. We chose to analyze sphingolipid metabolites due to recent evidence that modulation of this class of lipids can have therapeutic outcomes in models of type 2 diabetes (2–4). Despite this evidence of targeting sphingolipids as a therapy for type 2 diabetes, the actual changes to sphingolipid metabolites in type 1 diabetes have remained undefined until now. The major changes we observed in two distinct models of type 1 diabetes are: 1) an elevation of SoIP levels and 2) a selective decrease in nervonic acid-esterified sphingolipids in circulating plasma.

Changes in SoIP levels could have several implications for diabetes, in particular, cardiovascular disease. Research indicates that the heart and aorta from the STZ-induced diabetic rat have increased sphingosine kinase activity, which was diminished in animals given an insulin pump (18). Our data are consistent with previous research results because the

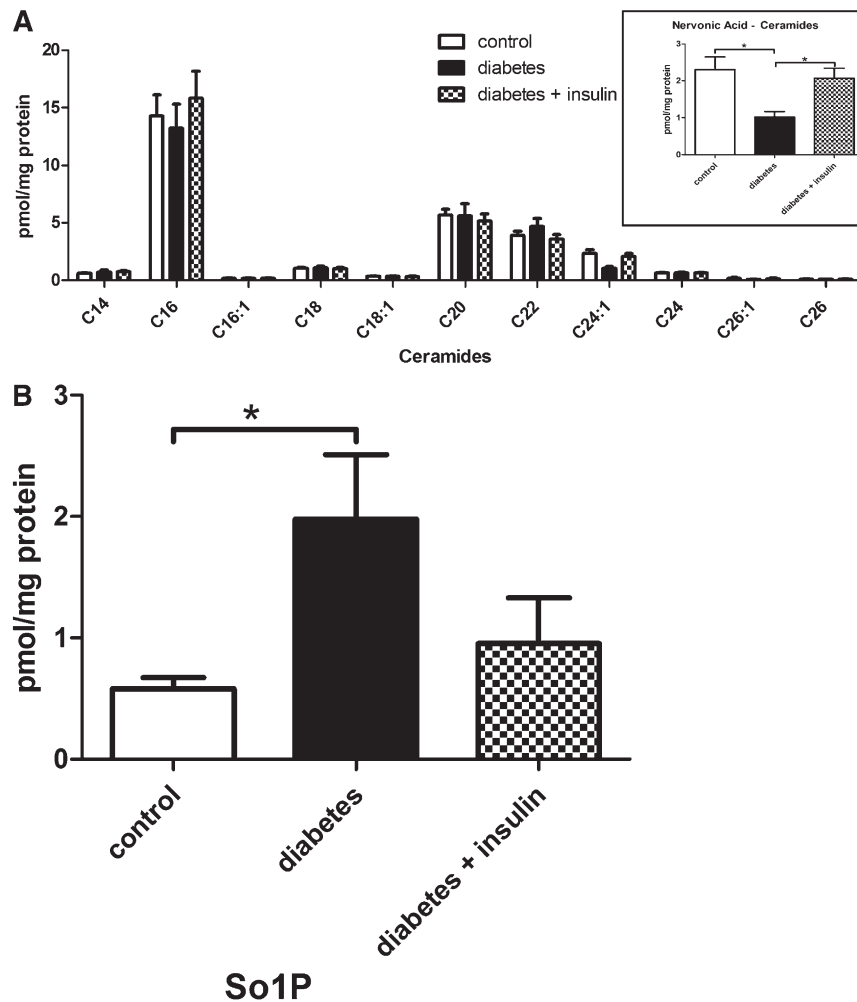


**Fig. 6.** Diabetes alters sphingolipid metabolites in the heart. Lipid extracts from the heart were analyzed for sphingolipids by LC-MS/MS. A: Ceramide species from control, *Ins2<sup>Akita</sup>*, and insulin-treated *Ins2<sup>Akita</sup>* groups are shown. 24:1 ceramides are depicted in the inset. B: Likewise, So1P mass was also assessed from the same animals. Data is presented as pmol/mg protein; n values are provided in Table 1. \* $P < 0.05$ .

product of sphingosine kinase, So1P, is elevated in the diabetic heart. Mechanistically, hyperglycemia induces sphingosine kinase activity and So1P levels, leading to enhanced leukocyte adhesion to endothelial cells and contributing to vascular damage (18). This high glucose induced-leukocyte adhesion to endothelial cells is blocked by overexpression of a kinase-dead sphingosine kinase 1 mutant (18), further implicating sphingosine kinase in diabetes-induced cardiovascular disease. Conversely, in KK/Ay diabetic mice, sphingosine kinase 1 gene delivery, via intravenous injection of adenoviruses, reduced blood glucose, led to reduced cholesterol, triglycerides, LDL, and nonesterified fatty acids, increased HDL, and prevented cardiac injury (19). So1P also prevented monocyte/endothelial interactions through activation of the So1P receptor,  $S1P_1$ , in the type 1 non-obese diabetic (NOD) mouse model (20). Analysis of circulating So1P in clinical samples demonstrates that So1P is more predictive of obstructive coronary artery disease than other well-established risk factors, including age, sex, family history, diabetes, lipid profile, and hypertension (16).

The complexity of the roles of So1P may have many underlying factors, including multiple sphingosine kinases, recep-

tors, and nonreceptor intracellular targets. These roles may have many effects depending on where So1P is localized in a cell. To add to its complexity, the  $S1P$  receptor,  $S1P_3$ , is involved in cardioprotection in in vivo ischemia/reperfusion models (21). The  $S1P_3$  receptor also has been implicated in regulating heart rate, and its activation results in bradycardia in both mice and humans (22–24). This controversy between the protective and detrimental actions of So1P and its targets has not yet been completely elucidated in diabetic models and represents a target of future investigation.

Another important finding of our type 1 diabetic study was a decrease in esterified nervonic acid in multiple sphingolipid classes, and this change could have significant implications for understanding diabetic complications. It has been reported that nervonic acid exerts a negative correlation on coronary risk factors and may have a preventive effect on metabolic disorders (17). Our data reveal that a high-fat diet also reduces nervonic acid, and that this nutritional stress can further decrease diabetes-induced reductions of nervonic acid. In addition, a reduction of nervonic acid-containing ceramides in diabetic cardiac tissue was also observed. The role of omega-9 fatty acids, such as nervonic

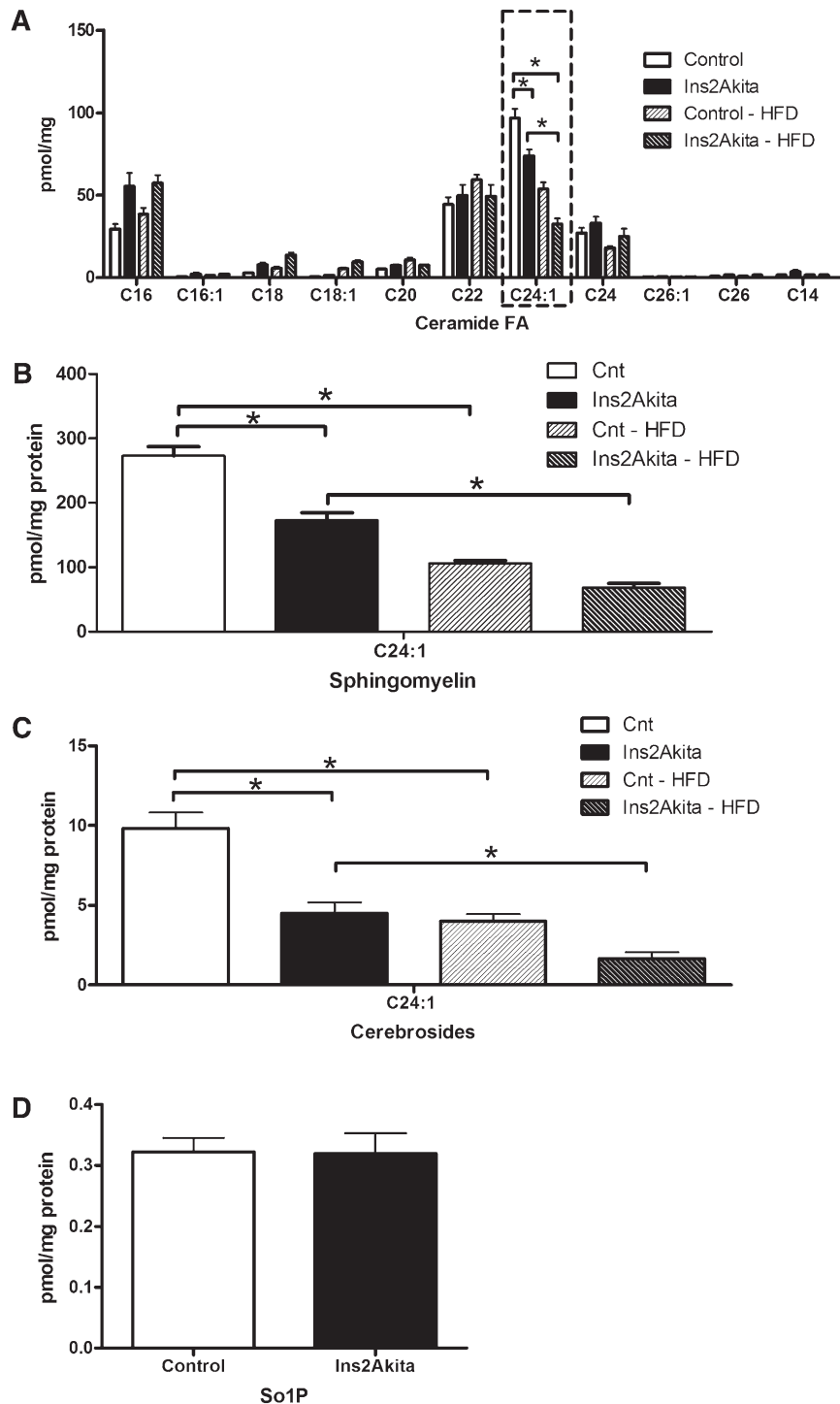


**Fig. 7.** Diabetes reduces 24:1 content in the liver. Lipids were extracted from the liver and assessed for sphingolipid content by LC-MS/MS. A: Ceramides from sibling controls and Ins2<sup>Akita</sup> diabetic mice on a low-fat or a high-fat diet were assessed. Similarly, 24:1-esterified sphingomyelin (B) and cerebrosides (C) were also determined. D: So1P content within normal and diabetic livers was also assessed. Data is presented as pmol/mg protein; n values are provided in Table 1. \* $P < 0.05$ .


acid, in maintaining health remains poorly defined. It is unclear whether nervonic acid exerts biophysical or biochemical properties associated with anti-inflammatory or protective actions. Also, the mechanism for diminished nervonic acid content remains unknown. It is intriguing that we observed decreases in several omega-9 precursor molecular species in

the diabetic plasma (e.g., C16:1, 18:1) from the total lipid pool, but these decreases are not evident in sphingolipids except for C24:1. Diabetes has been demonstrated to impair/alter fatty acid elongases and fatty acid desaturases. Specifically, the elongase ELOVL6 and delta-9 desaturase (enzymes responsible for the synthesis of omega-9 C16:1 and



C18:1 fatty acids and precursors to nervonic acid) can be inhibited by diabetes or a high-fat diet (25), which could explain the reduction observed in the diabetic plasma.

In addition to cardiovascular disease, diminished nervonic acid may also influence diabetic neuropathy. Diminished nervonic acid has been observed in demyelinating diseases such as multiple sclerosis and adrenoleukodystrophy (26). Demyelination also occurs in peripheral neuropathy in diabetes (27), and supplementation of nervonic acid in diabetic patients could potentially mitigate the deleterious complications of this condition.

Sphingolipid metabolism in various tissues can respond differently to diabetes. For instance, although the SoIP levels increased in the heart and plasma, the diabetic liver did not demonstrate a change. We also have previously published studies showing elevated glucosylceramide at the expense of ceramide in the retina (6), and others have shown a similar pattern in the kidneys (28). We, however, did not observe this phenomenon in the plasma. Therefore, a better understanding of systemic sphingolipid metabolism is needed, especially in regard to altered content in organs associated with diabetic complications. Taken together, our studies have identified novel diabetes-induced alterations in circulating sphingolipids, as evidenced by an increase in the putatively pro-inflammatory SoIP and a reduction in cardio- and neuro-protective esterified nervonic acid. These changes could potentially mediate diabetes-induced systemic disease, such as inflammation, and influence peripheral complications, including cardiovascular disease and neuropathy. 

## REFERENCES

1. Fox, T. E., and M. Kester. 2010. Therapeutic strategies for diabetes and complications: a role for sphingolipids? *Adv. Exp. Med. Biol.* **688**: 206–216.
2. Holland, W. L., J. T. Brozinick, L. P. Wang, E. D. Hawkins, K. M. Sargent, Y. Liu, K. Narra, K. L. Hoehn, T. A. Knotts, A. Siesky, et al. 2007. Inhibition of ceramide synthesis ameliorates glucocorticoid-, saturated-fat-, and obesity-induced insulin resistance. *Cell Metab.* **5**: 167–179.
3. Aerts, J. M., R. Ottenhoff, A. S. Powlson, A. Grefhorst, M. van Eijk, P. F. Dubbelhuis, J. Aten, F. Kuipers, M. J. Serlie, T. Wennekes, et al. 2007. Pharmacological inhibition of glucosylceramide synthesis enhances insulin sensitivity. *Diabetes.* **56**: 1341–1349.
4. Zhao, H., M. Przybylska, I. H. Wu, J. Zhang, C. Siegel, S. Komarnitsky, N. S. Yew, and S. H. Cheng. 2007. Inhibiting glycosphingolipid synthesis improves glycemic control and insulin sensitivity in animal models of type 2 diabetes. *Diabetes.* **56**: 1210–1218.
5. Hong, E. G., D. Y. Jung, H. J. Ko, Z. Zhang, Z. Ma, J. Y. Jun, J. H. Kim, A. D. Sumner, T. C. Vary, T. W. Gardner, et al. 2007. Nonobese, insulin-deficient Ins2Akita mice develop type 2 diabetes phenotypes including insulin resistance and cardiac remodeling. *Am. J. Physiol. Endocrinol. Metab.* **293**: E1687–E1696.
6. Fox, T. E., X. Han, S. Kelly, A. H. Merrill 2nd, R. E. Martin, R. E. Anderson, T. W. Gardner, and M. Kester. 2006. Diabetes alters sphingolipid metabolism in the retina: a potential mechanism of cell death in diabetic retinopathy. *Diabetes.* **55**: 3573–3580.
7. Merrill, A. H., Jr., M. C. Sullards, J. C. Allegood, S. Kelly, and E. Wang. 2005. Sphingolipidomics: high-throughput, structure-specific, and quantitative analysis of sphingolipids by liquid chromatography-tandem mass spectrometry. *Methods.* **36**: 207–224.
8. Wijesinghe, D. S., J. C. Allegood, L. B. Gentile, T. E. Fox, M. Kester, and C. E. Chalfant. 2010. Use of high performance liquid chromatography-electrospray ionization-tandem mass spectrometry for the analysis of ceramide-1-phosphate levels. *J. Lipid Res.* **51**: 641–651.
9. Martin, R. E., M. H. Elliott, R. S. Brush, and R. E. Anderson. 2005. Detailed characterization of the lipid composition of detergent-resistant membranes from photoreceptor rod outer segment membranes. *Invest. Ophthalmol. Vis. Sci.* **46**: 1147–1154.
10. Zeidan, Y. H., and Y. A. Hannun. 2007. Translational aspects of sphingolipid metabolism. *Trends Mol. Med.* **13**: 327–336.
11. Yoshioka, M., T. Kayo, T. Ikeda, and A. Koizumi. 1997. A novel locus, Mody4, distal to D7Mit189 on chromosome 7 determines early-onset NIDDM in nonobese C57BL/6 (Akita) mutant mice. *Diabetes.* **46**: 887–894.
12. Brunengraber, D. Z., B. J. McCabe, T. Kasumov, J. C. Alexander, V. Chandramouli, and S. F. Previs. 2003. Influence of diet on the modeling of adipose tissue triglycerides during growth. *Am. J. Physiol. Endocrinol. Metab.* **285**: E917–E925.
13. Kim, J. K., H. J. Kim, S. Y. Park, A. Cederberg, R. Westergren, D. Nilsson, T. Higashimori, Y. R. Cho, Z. X. Liu, J. Dong, et al. 2005. Adipocyte-specific overexpression of FOXC2 prevents diet-induced increases in intramuscular fatty acyl CoA and insulin resistance. *Diabetes.* **54**: 1657–1663.
14. Weisberg, S. P., D. McCann, M. Desai, M. Rosenbaum, R. L. Leibel, and A. W. Ferrante, Jr. 2003. Obesity is associated with macrophage accumulation in adipose tissue. *J. Clin. Invest.* **112**: 1796–1808.
15. Xu, H., G. T. Barnes, Q. Yang, G. Tan, D. Yang, C. J. Chou, J. Sole, A. Nichols, J. S. Ross, L. A. Tartaglia, et al. 2003. Chronic inflammation in fat plays a crucial role in the development of obesity-related insulin resistance. *J. Clin. Invest.* **112**: 1821–1830.
16. Deutschman, D. H., J. S. Carstens, R. L. Klepper, W. S. Smith, M. T. Page, T. R. Young, L. A. Gleason, N. Nakajima, and R. A. Sabbadini. 2003. Predicting obstructive coronary artery disease with serum sphingosine-1-phosphate. *Am. Heart J.* **146**: 62–68.
17. Oda, E., K. Hatada, J. Kimura, Y. Aizawa, P. V. Thanikachalam, and K. Watanabe. 2005. Relationships between serum unsaturated fatty acids and coronary risk factors: negative relations between nervonic acid and obesity-related risk factors. *Int. Heart J.* **46**: 975–985.
18. Wang, L., X. P. Xing, A. Holmes, C. Wadham, J. R. Gamble, M. A. Vadas, and P. Xia. 2005. Activation of the sphingosine kinase-signaling pathway by high glucose mediates the proinflammatory phenotype of endothelial cells. *Circ. Res.* **97**: 891–899.
19. Ma, M. M., J. L. Chen, G. G. Wang, H. Wang, Y. Lu, J. F. Li, J. Yi, Y. J. Yuan, Q. W. Zhang, J. Mi, et al. 2007. Sphingosine kinase 1 participates in insulin signalling and regulates glucose metabolism and homeostasis in KK/Ay diabetic mice. *Diabetologia.* **50**: 891–900.
20. Whetzel, A. M., D. T. Bolick, S. Srinivasan, T. L. Macdonald, M. A. Morris, K. Ley, and C. C. Hedrick. 2006. Sphingosine-1 phosphate prevents monocyte/endothelial interactions in type 1 diabetic NOD mice through activation of the S1P1 receptor. *Circ. Res.* **99**: 731–739.
21. Means, C. K., C. Y. Xiao, Z. Li, T. Zhang, J. H. Omens, I. Ishii, J. Chun, and J. H. Brown. 2007. Sphingosine 1-phosphate S1P2 and S1P3 receptor-mediated Akt activation protects against in vivo myocardial ischemia-reperfusion injury. *Am. J. Physiol. Heart Circ. Physiol.* **292**: H2944–H2951.
22. Sanna, M. G., J. Liao, E. Jo, C. Alfonso, M. Y. Ahn, M. S. Peterson, B. Webb, S. Lefebvre, J. Chun, N. Gray, et al. 2004. Sphingosine 1-phosphate (S1P) receptor subtypes S1P1 and S1P3, respectively, regulate lymphocyte recirculation and heart rate. *J. Biol. Chem.* **279**: 13839–13848.
23. Forrest, M., S. Y. Sun, R. Hajdu, J. Bergstrom, D. Card, G. Doherty, J. Hale, C. Keohane, C. Meyers, J. Milligan, et al. 2004. Immune cell regulation and cardiovascular effects of sphingosine 1-phosphate receptor agonists in rodents are mediated via distinct receptor subtypes. *J. Pharmacol. Exp. Ther.* **309**: 758–768.
24. Budde, K., R. L. Schmuuder, R. Brunkhorst, B. Nashan, P. W. Lucker, T. Mayer, S. Choudhury, A. Skerjanec, G. Kraus, and H. H. Neumayer. 2002. First human trial of FTY720, a novel immunomodulator, in stable renal transplant patients. *J. Am. Soc. Nephrol.* **13**: 1073–1083.
25. Wang, Y., D. Botolin, J. Xu, B. Christian, E. Mitchell, B. Jayaprakasam, M. G. Nair, J. M. Peters, J. V. Busik, L. K. Olson, et al. 2006. Regulation of hepatic fatty acid elongase and desaturase expression in diabetes and obesity. *J. Lipid Res.* **47**: 2028–2041.
26. Sargent, J. R., K. Coupland, and R. Wilson. 1994. Nervonic acid and demyelinating disease. *Med. Hypotheses.* **42**: 237–242.
27. Sharma, K. R., J. Cross, O. Farronay, D. R. Ayyar, R. T. Shebert, and W. G. Bradley. 2002. Demyelinating neuropathy in diabetes mellitus. *Arch. Neurol.* **59**: 758–765.
28. Zador, I. Z., G. D. Deshmukh, R. Kunkel, K. Johnson, N. S. Radin, and J. A. Shayman. 1993. A role for glycosphingolipid accumulation in the renal hypertrophy of streptozotocin-induced diabetes mellitus. *J. Clin. Invest.* **91**: 797–803.